Journal of the European Ceramic Society **15** (1995) 1007–1014

0955-2219(95)00077-1
0955-2219/95/$9.50

Effect of Gaseous Environment on the Corrosion of β-Sialon Materials

R. Ramesh,[a] M. J. Pomeroy,[a] H. Chu[b] & P. K. Datta[b]

[a]Department of Materials Science and Technology, University of Limerick, Limerick, Ireland
[b]Department of Mechanical Engineering and Manufacturing Systems, University of Northumbria at Newcastle, Ellison Building, Ellison Place, Newcastle upon Tyne, UK.

(Recieved 28 June 1994; revised version received 26 April 1995; accepted 16 May 1995)

Abstract

This paper reports the effects of different gaseous environments on the corrosion behaviour of β*-sialon materials. Six* β*-sialon materials with* z*-values of 0·2, 0·5, 1·0, 1·5, 2·0 and 3·0 were prepared by pressureless sintering. Corrosion results obtained at 1350°C in environments comprising (i) Laboratory air; (ii) Argon – 20% oxygen – 2% chlorine; (iii) hydrogen – 10% hydrogen sulphide – 2% water vapour and (iv) nitrogen – 15% carbon dioxide – 4% oxygen – 0·2% sulphur dioxide showed that for each of the four environments the* z *= 3·0 material exhibited the best corrosion resistance. The mechanism of corrosion at 1350°C in each of the four environments involves the formation of large volumes of low viscosity liquid phases. These large volumes of liquid enable the solution of* β*-sialon grains to occur and it is this process which is responsible for corrosion.*

1 Introduction

There are a wide range of fossil fuel conversion systems, eg. coal gasifiers, conventional and advanced coal-fired power generation systems and industrial incinerators where silicon nitride components may afford cycle efficiency increases due to either the employment of higher cycle temperatures or the obviation of inefficient component cooling. Whilst the excellent oxidation resistance of silicon nitride materials has been documented[1] and the effects of condensed sodium sulphate deposits assessed[2] no significant body of literature exists relating to the corrosion of such materials in gaseous environments typifying coal gasifiers, conventional/advanced power generation plant and waste incinerators. Oxychlorine and sulphur containing environments, which normally prevail in such industrial processes, can cause accelerated corrosion through the formation of volatile oxychlorides,[3,4] and SiS/SiO compounds,[5] respectively.

The corrosion of silicon based ceramics in corrosive gases at high temperatures has been investigated but it has been mainly confined either to hot pressed or hot isostatically pressed materials. The oxidation of such silicon nitride materials has been shown to be strongly dependent on the level of oxidant in the ambient gases.[6,7] When a high level of oxidant is present, a protective silicate layer is formed which separates the underlying ceramic from the environment. Oliveira *et al.*[5] defined the limits of pO_2 and pS_2 and temperature for the safe usage of hot pressed/HIPped silicon nitride by testing in gas mixtures similar to those that are likely to be encountered in coal gasifiers. An assessment of the effect of similar environments on the mechanical behaviour has also been made for hot pressed silicon nitride materials.[8] In contrast, no significant body of information is available for pressureless sintered materials.

The corrosion of silicon nitrides by gases representative of flue gases emanating from gas-, oil- or coal-fired combustion plant has not been directly studied. However, Demaison, *et al.*[9] have compared the corrosion of two similar β-sialon materials in oxygen and carbon dioxide. The results obtained by Demaison *et al.* indicate that the carbon dioxide environment encourages the development of oxide scales which are considerably more fluid than those which form during corrosion.

In studying the corrosion of materials by aggressive media it is important to understand the process by which simple oxidation takes place. The mechanism by which the oxidation of silicon-nitride based materials occurs is thus important and has been shown to depend upon temperature.[10,11] For temperatures typically in the range 1000–1150°C oxygen diffusion across a protective silica layer is rate controlling. For higher temperatures (up to 1400°C) the diffusion of sintering

additive cations and impurities from the interior of the ceramic into the surface silicon rich oxide scale is considered to be the rate controlling step. The rate controlling step in the mechanism by which silicon nitride oxidises at even higher temperatures has not been fully elucidated. In the intermediate temperature range, oxidation rates as determined from straight line relationships between the square of specific weight gain and time are observed to depend on the type and level of additives employed during sintering.[10–12] This is unfortunate since additive types and levels which facilitate pressureless sintering give rise to accelerated oxidation. One exception to this general rule is the oxidation behaviour of certain sialon materials.[12] In addition, attention has been drawn to the fact that additive rich oxide liquids, possibly containing nitrogen, are formed during the oxidation process.[9,13] Whether or not the formation of such liquids is an effect of the oxidation process or its cause has not been fully rationalised even though it is clear that the formation of such liquids and their volume is dependent on the diffusion of additive and impurity cations into the surface scales.

The research presented in this paper addresses the effect of the z-value of pressureless sintered β-sialons ($Si_{(6-z)}Al_zO_zN_{(8-z)}$) on the corrosion of these ceramics in environments typical of those arising in coal conversion and waste incineration plants.

2 Experimental Detail

The starting compositions of the materials employed in this work are given in Table 1 together with theoretical densities achieved and phase assemblages observed after firing. Weighed amounts of the relevant powders were ball milled for 24 h under isopropanol in a polypropylene container using sialon milling media. The mixtures were then homogenised for 30 min, dried and sieved to <212 μm. They were then cold isostatically pressed at 2000 atm. in a rubber mould. The cold pressed bars, typically 15 × 15 × 50 mm, were then located in a powder bed (50:50 boron nitride:silicon nitride) which was contained in an alumina crucible. The bars were then fired for 2 h at 1700°C in flowing nitrogen. The fired densities were measured by the Archimedes principle using both water and mercury as working fluids. The densities observed were compared with theoretical densities derived from the mass fractions and densities of the relevant sialon and Y–Si–Al–O–N glass phases present in the ceramic. The phase assemblages of the fired materials were determined using X-ray diffraction (XRD) and the z-value of the sialon ceramics determined using correlations and data published by Ekstrom *et al.*[14]

Following fabrication, corrosion experiments were performed in tube furnaces using specimens typically 10 × 10 × 3 mm, polished to a 1 μm finish. A heating and cooling rate of 8°C min^{-1} was employed for each experiment.

Corrosion experiments were conducted in different gaseous environments under the following conditions for all the materials chosen:

(1) Laboratory air at a temperature of 1350°C for 128 h.
(2) A chloridising environment comprising argon – 2% chlorine, 20% oxygen at a temperature of 1350°C for 100 h.
(3) A sulphidising environment comprising hydrogen – 10% hydrogen sulphide – 2% water vapour at a temperature of 1350°C for 100 h.
(4) A simulated flue gas environment comprising nitrogen – 15% carbon dioxide, 4% oxygen, 0·2% sulphur dioxide at a temperature of 1350°C for 96 h.

Corroded coupons were weighed following their removal from the relevant environment and extents of corrosion expressed as weight gain per unit area, i.e. specific weight gain. For materials exposed to the chloridising and sulphidising environments thickness loss measurements were used to assess extents of corrosion because weight losses were observed to occur in certain instances as stated below. The phase assemblage of the surface layers of the corrosion scales was determined using XRD and the surface morphology using scanning electron microscopy (SEM). Large

Table 1. Compositions (wt%), densities and phase assemblage for materials

Nominal z-value	Y_2O_3	Si_3N_4	*AlN*	Al_2O_3	*% theor. density*	*% β-sialon*	*Analysed z-value*	*Other phases*
0·2	7·00	87·98	0·65	4·37	96	100	0·22	none
0·5	7·03	83·33	1·73	7·91	98	100	0·54	none
1·0	7·08	75·59	3·53	13·80	98	100	0·85	none
1·5	7·13	67·50	5·16	20·21	98	100	—	none
2·0	7·18	60·17	7·13	25·52	98	100	2·05	none
3·0	7·28	44·82	10·70	37·20	100	100	2·70	YAG

All compositions are based on 88·9 v/o of relevant sialon–11·1 v/o Y-sialon glass of composition (in equivalent %) 28 Y; 56 Si; 16 Al; 80 O; 20 N.

(1·6 × 1·0 mm) energy dispersive X-ray analyses (EDX) of the surface layers of selected specimens were conducted in order to determine the cation (Y, Al, Si) compositions of these scales.

3 Results

3.1 Fabrication and phase assemblage

From the results presented in Table 1, it is seen that as the nominal z-value of the materials increases, greater densification occurs during firing. The data shown in Table 1 also shows that full conversion of the α-silicon nitride powder to β-sialon occurs during firing. In only one instance (z = 3·0 matrix) was a residual crystalline phase observed. This phase was yttrium aluminium garnet and it is thought that the formation of this phase contributes to the discrepancy between nominal and observed z-value. For other compositions the z-values determined from the lattice parameter shifts agree fairly well with the nominal values.

3.2 Corrosion

3.2.1 Laboratory air

The variation in weight gain as measured after 128 h at 1350°C shows that z-values in the intermediate range ($0{\cdot}5 \geq z \leq 1{\cdot}5$) are the least resistant to oxidation at 1350°C (Fig. 1). The phase assemblages as identified by XRD indicate yttrium disilicate or cristobalite as the major surface phases for the z = 0·2–1·0 materials, while for the higher z-value materials mullite is the predominant phase. Typical surface textures observed for the z = 0·2, 1·0 and 2·0 materials are shown in Fig. 2. As can be seen, both z = 0·2 and 2·0 materials show a marked level of crystallinity in terms of yttrium disilicate and needle like mullite crystals respectively. The z = 1·0 material is typified by the occurrence of needle like mullite crystals and a grey cristobalite phase located in an amorphous phase. Superposition of the large area surface analyses on the Y_2O_3–SiO_2–Al_2O_3 phase diagram[15] showed that for the z = 0·2 and 0·5 materials the compositions lay in the yttrium disilicate–silica–eutectic phase field. For the z = 1·0, 1·5, 2·0 and 3·0 the compositions lay within the mullite–silica–eutectic phase field. Indeed the surface compositions for the latter three materials lay on a line joining the eutectic and mullite.

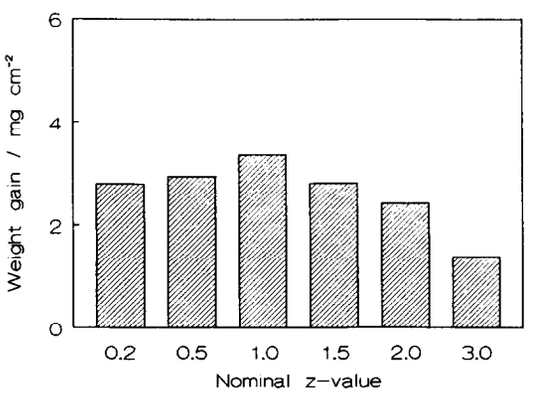

Fig. 1. Weight change data as a function of z-value after 128 h oxidation at 1350°C.

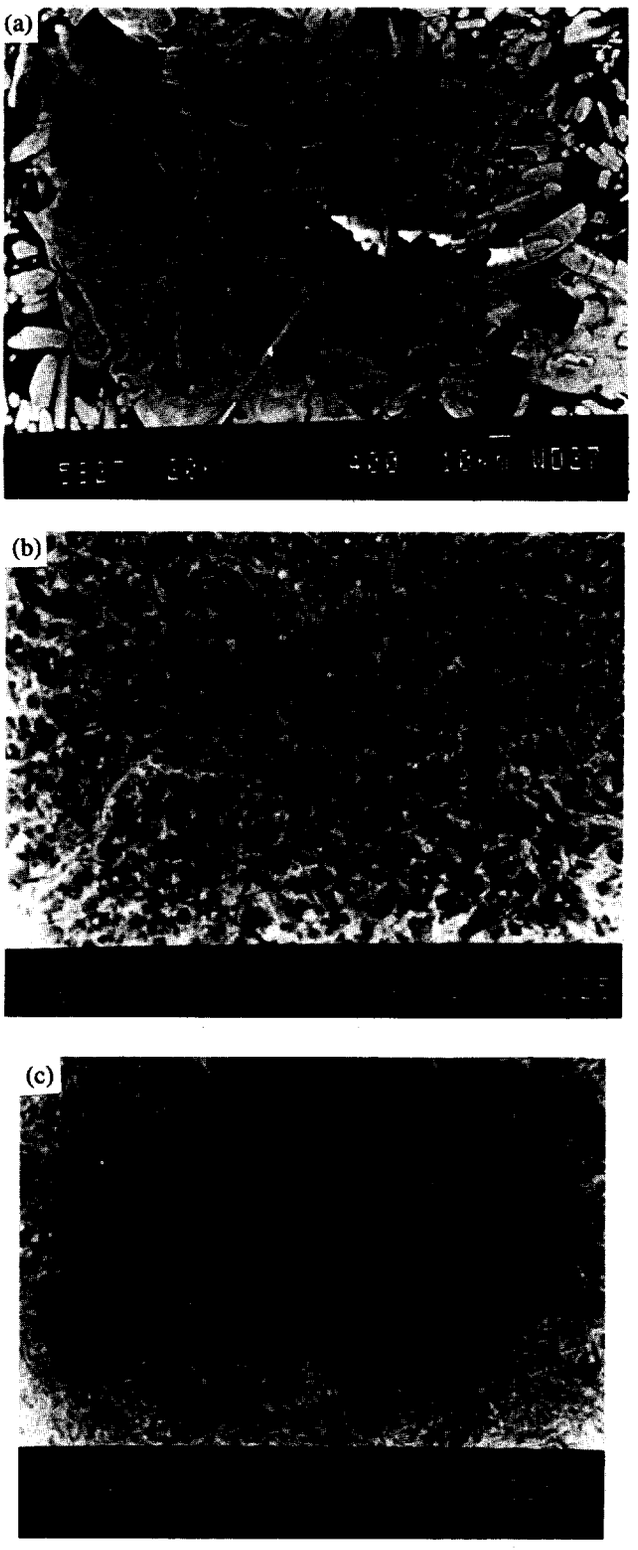

Fig. 2. Surface morphology of oxidation products formed on β-sialon materials after 128 h oxidation at 1350°C (a) z = 0·2, (b) z = 1·0 and (c) z = 2·0.

3.2.2 Chloridation environment

Figure 3 shows the weight change data for $z = 0{\cdot}2$ material following exposure to $2\%Cl_2/20\%O_2/Ar$ gas mixture at 1350°C for time periods up to 100 h. It is seen from this figure that the specific weight gain increases with time up to 50 h duration and then decreases for longer time periods. This decrease in weight gain was considered to be due to the volatilisation of corrosion products as most chloride and oxychloride reaction products are volatile at elevated temperatures.[16] Similar effects were observed in the sulphidising environments. Accordingly, it was decided that the use of specific weight change data as a measure of corrosion could be erroneous and hence thickness loss measurements were subsequently used to establish extents of corrosion after 100 h exposure. Figure 4 shows thickness loss data obtained for the β-sialons of different z values exposed to the argon – 20% oxygen – 2% chlorine environment at 1350°C. It is seen that as z-value increases the extent of corrosion after 100 h initially increases with z-value and then decreases. The most corrosion resistant material is that with a z-value of 3·0.

The morphology of the corrosion scales formed after 100 h corrosion was observed to be dependent on z-value. The scales were amorphous for materials with z-values of 0·2, 0·5, 1·0 and 1·5. For the $z = 2{\cdot}0$ material sillimanite and mullite

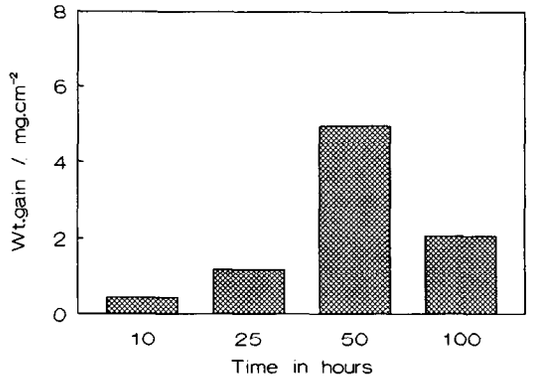

Fig. 3. Weight gain–time relationship for z = 0·2 sialon exposed to $2\%Cl_2/20\%O_2/Ar$ mixture at 1350°C.

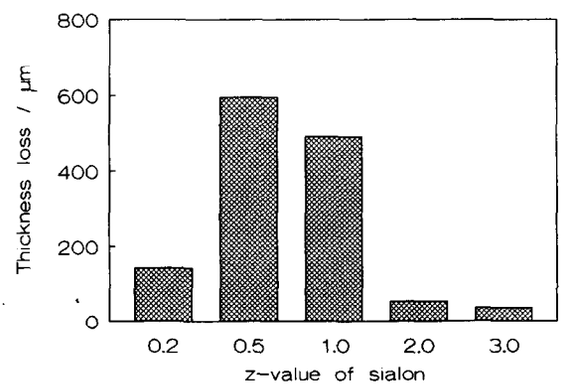

Fig. 4. Thickness loss data obtained for different sialon materials exposed to chloridising environment for 100 h at 1350°C.

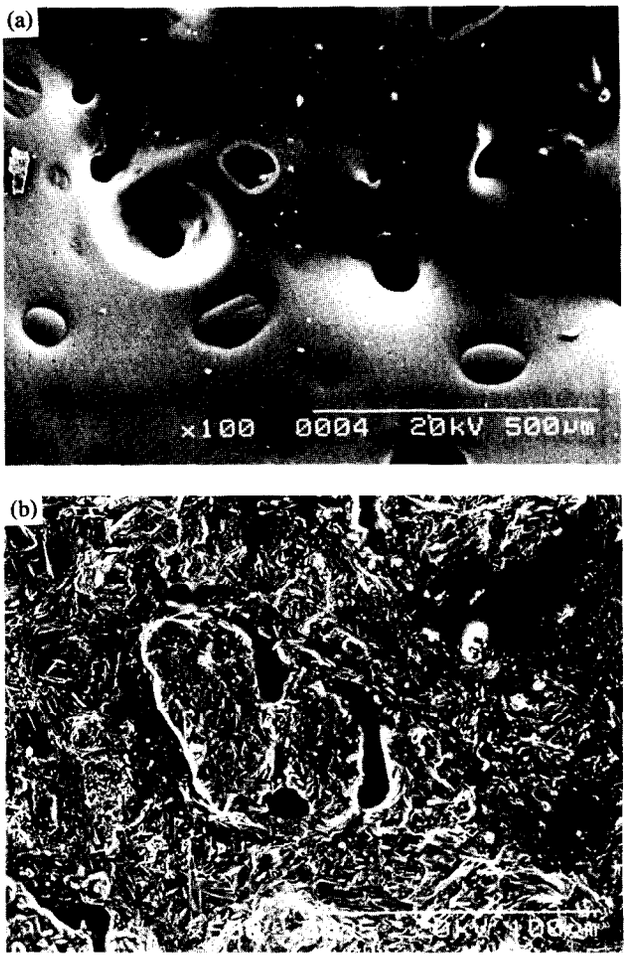

Fig. 5. Surface morphologies of the corrosion products formed following exposure to $2\%Cl_2/20\%O_2/Ar$ gas mixture at 1350°C (a) $z = 1{\cdot}0$ and (b) $z = 3{\cdot}0$.

crystals were observed in an amorphous scale and mullite crystals were observed to be present in an amorphous scale in the case of the $z = 3{\cdot}0$ material. Figure 5 shows representative surface morphologies of the corrosion products formed on the $z = 1{\cdot}0$ and 3·0 materials.

3.2.3 Sulphidising environment

The effect of z-value on corrosion thickness loss in the $H_2 - 10\%\ H_2S - 2\%H_2O$ environment is shown in Fig. 6. This figure shows that the extent of

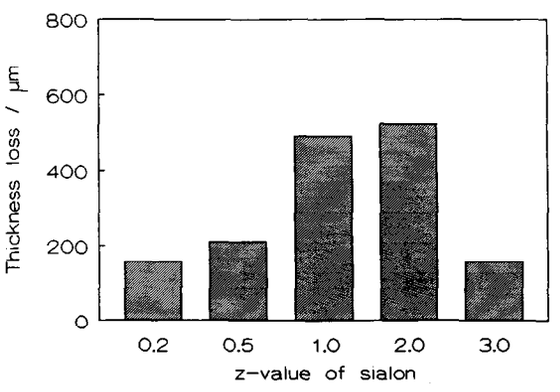

Fig. 6. Thickness loss data obtained for different sialon materials exposed to sulphidising environment for 100 h at 1350°C.

corrosion increases with increasing z-value up to 2·0 and then decreases with z = 0·2 and 3·0 materials undergoing least corrosion. The phase assemblages and surface morphologies observed for the different materials were similar to those observed for the chloridising environment.

3.2.4 Simulated flue gas environment

The form of the specific weight gain–time curve obtained for the z = 0·2 material exposed to the simulated flue gas environment at 1350°C was parabolic with rates of weight gain diminishing with time. Accordingly, it was assumed that no weight losses occurred during 96 h exposure and that weight gain data gave a true reflection of extent of corrosion. Figure 7 shows specific weight gain data as a function of z-value after exposure for 96 h at 1350°C. It is seen from this figure that as z-value increases from 0·2 to 1·0 the extents of corrosion increase. For z-values in excess of 1·0, the extent of corrosion decreases with increasing z-value.

The phase assemblages of the surface layers were observed to dependent on z-value. For the z = 0·2 material the predominant phase formed was β-yttrium disilicate which coexisted with silica and γ-yttrium disilicate. For the z = 0·5 material the predominant phase in the surface layers was silica. For the z = 1·0, 2·0 and 3·0 materials the predominant phase formed was mullite. Silica was also observed for these materials. A comparison of the amounts of liquid formed in the simulated flue gas environment with those formed during oxidation of similar materials for a similar length of time showed that the presence of carbon dioxide and sulphur dioxide in the simulated flue gas encouraged liquid formation (Fig. 8). The surface morphology of the z = 0·5 material exposed to the simulated flue gas environment for 48 h at 1350°C shown in Fig. 8 clearly demonstrates the occurrence of a large volume of liquid on the surface of the corroding sialon. The bright crystals seen in both Fig. 8 (a) and (b) are yttrium disilicate. z = 3·0 materials exhibit little liquid formation (Fig. 9) and this is consistent with the lowest corrosion rates observed (Fig. 7). Furthermore, large scale EDX analyses showed that for the low z-value materials (z = 0·2, 0·5 and 1·0) the surface layers of the corrosion scales formed in the simulated flue gas environment were richer in aluminium than

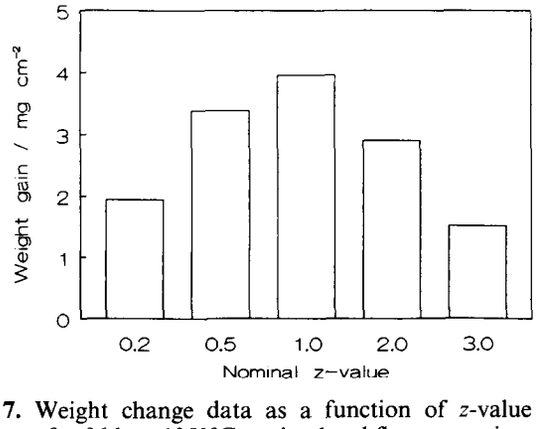

Fig. 7. Weight change data as a function of z-value after exposure for 96 h at 1350°C to simulated flue gas environment.

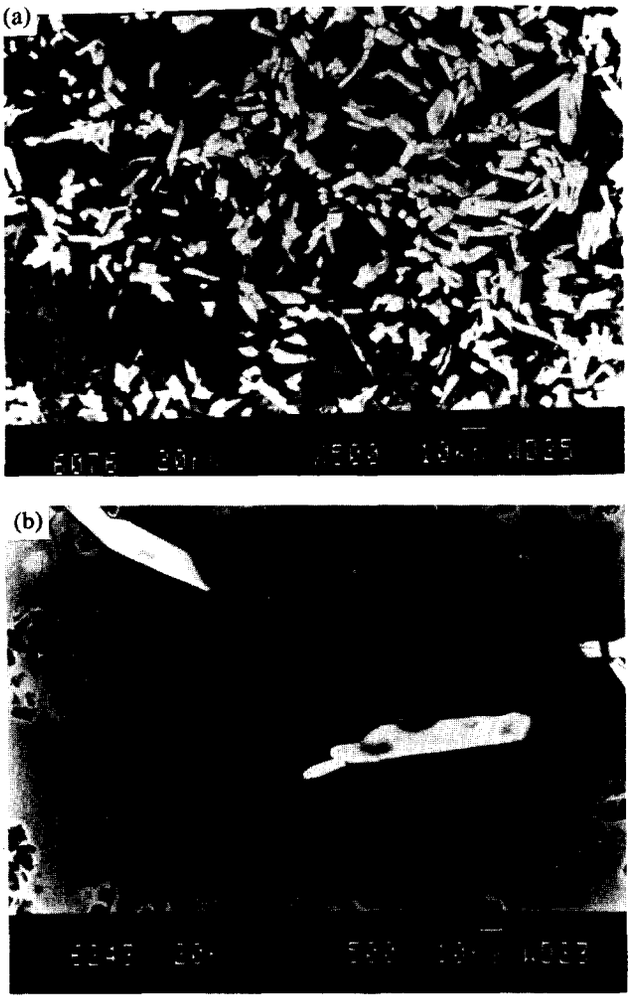

Fig. 8. Surface morphology of 0·5 sialon material after 48 h exposure at 1350°C in (a) laboratory air environment and (b) simulated flue gas environment.

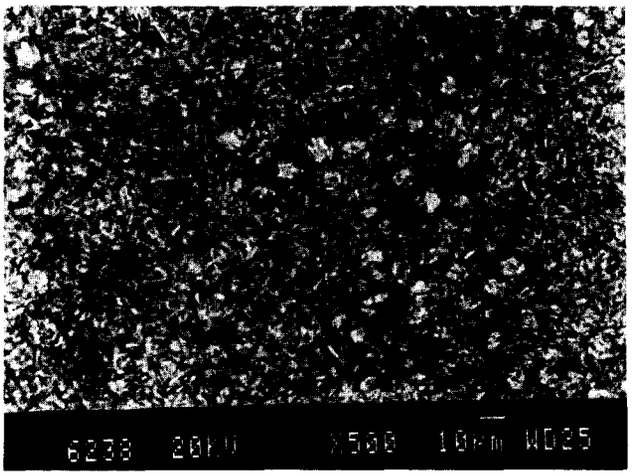

Fig. 9. Surface morphology of 3·0 sialon material after 48 h exposure at 1350°C in simulated flue gas environment.

those formed during oxidation. It is to be noted however that the crystalline phases formed were the same in both environments.

4 Discussion of Results

4.1 Relative corrosion resistance

Of the materials tested the $z = 3{\cdot}0$ material appears to be the most resistant to oxidation/corrosion by laboratory air. This material is also without doubt the most corrosion resistant material in the other three environments used in this work. The fact that the mullite forming $z = 3{\cdot}0$ material exhibits little liquid formation during corrosion in any of the environments investigated is most probably the reason for its excellent corrosion behaviour. In general the $z = 1{\cdot}0$ material undergoes the most extensive corrosion in each of the four environments studied.

4.2 Effect of environment on corrosion scales developed

From the results presented above it is clear that liquid phases are formed on the surfaces of the materials investigated during exposure to laboratory air. In the chloridising environment, chlorine is the only reactive gas addition which can account for the accelerated oxidation and significant extent of corrosion observed. In addition, the extent of liquid phase formation is greater in the chloridising environment than the laboratory air environment; indeed the scales formed on the $z = 0{\cdot}2$, $0{\cdot}5$, $1{\cdot}0$ and $1{\cdot}5$ materials are wholly amorphous. It is to be expected that the corrosion scales formed in the chloridising environment are more fluid than those formed in laboratory air since Hetherington *et al.*[17] noted marked decreases in the viscosity of fused silica contaminated with trace amounts of chlorine. In the case of the sulphidising environment the situation is more complex since both hydrogen and sulphur vapour are present in addition to the oxygen provided as water vapour. In order to ascertain the exact effect of hydrogen sulphide on the corrosion process, additional experiments were conducted at 1350°C in a gaseous environment comprising hydrogen–2% water vapour using the $z = 0{\cdot}2$ material. The results obtained from this work demonstrated that the corrosion rate was less than that observed for the environment containing hydrogen sulphide and that the corrosion products showed some crystallinity. It may therefore be concluded that the large volumes of low viscosity liquid formed in the sulphidising environment, compared to those formed in laboratory air, arise from the synergistic effects of hydrogen and sulphur. Combining the findings of Demaison *et al.*[9] and the results obtained for the simulated flue gas environment strongly suggests that carbon dioxide and sulphur dioxide exert a similar synergistic effect on liquid volume and viscosity. This is clearly demonstrated by comparison of the micrographs shown in Figs. 8(a) and (b). As stated above, the exterior layers of the corrosion scales formed on the $z = 0{\cdot}2$ and $0{\cdot}5$ materials in the simulated flue gas environment were observed to contain more aluminium than those formed in the laboratory air environment. Since the crystalline phases formed ($Y_2Si_2O_7$ and SiO_2) do not contain this element, more liquid is expected to form in the former environment as observed above.

4.3 Corrosion mechanisms

Combining the above rationalisation of the effects of environment on the volume and fluidity of liquid corrosion products with the extents of oxidation and corrosion suffered by the different sialon materials indicates that for large volumes of a fluid corrosion product, (i.e. chloridising and sulphidising environments) extents of corrosion are significantly greater than those observed when lower volumes of liquid are formed, (i.e. simulated flue gas and oxidising environments). This correlation indicates that the role played by liquids in the oxidation and corrosion mechanisms operating at 1350°C is extremely important. Additional experiments with RBSN have shown that the $\beta/(\alpha + \beta)$ silicon nitride ratio observed in the layers beneath the cristobalite corrosion product formed in the simulated flue gas environment is greater than in the starting material. It was also observed that in addition to cristobalite a calcium containing amorphous phase was present in the surface layers of the corrosion product. In order for the α-/β-phase transformation to occur, a liquid phase must be present to facilitate the solution–precipitation reaction.[18] It would therefore appear that α-silicon nitride is dissolved by the calcium containing liquid present at 1350°C and reprecipitated as β-silicon nitride. This finding suggests that silicon nitride can be dissolved by liquid corrosion products. In order to validate the fact that the α/β transformation could occur at such a low temperature a green sample of the $z = 0{\cdot}2$ material was sintered for 96 h in flowing nitrogen at a temperature of 1350°C. The density of the material increased from 62% of theoretical to 90% and the initial β-content of 5% increased to 65% clearly demonstrating that densification and associated solution–precipitation effects could occur over long time periods at 1350°C. If α-silicon nitride can dissolve in a liquid corrosion product it seems plausible to assume that β-silicon nitride and sialons can also. However, dissolved β-silicon

nitride and β-sialons cannot be reprecipitated as α. Accordingly, if the β-silicon nitride dissolves in the corrosion scale it is likely that the resulting nitrogen saturated liquid will decompose into a liquid containing little nitrogen and the relevant crystalline silicates or silica. If this mechanism of oxidation and corrosion is accepted then the rate of corrosion should be dependent on the volume and viscosity of the liquid formed during oxidation. Greater liquid volumes will result in greater extents of silicon nitride/sialon solution and lower viscosities will enable the dissolution products to be transported away from the liquid – nitride interface more rapidly. The extensive corrosion of the various materials in the chloridising and sulphidising environments is thus easy to comprehend.

As stated in the introduction, although rates of oxidation at temperatures of the order of 1350°C are controlled by the diffusion rate of additive and impurity cations from the bulk of the ceramic into the surface scale the exact reasons for this are not fully appreciated. The above arguments relating to corrosion mechanisms enable a fuller appreciation to be put forward if it is realised that the diffusion of additive and cation impurities into the surface scale increases its liquid content and lowers the viscosity of the liquid formed. Such an argument is consistent with observations that the type and level of additive employed during densification control oxidation rate[11,12] since additive types and levels which give rise to large volumes of low viscosity liquids during densification will give rise to large quantities of low viscosity liquids in oxide scales.

In designing silicon nitride ceramics for high temperature corrosion resistant applications the selection of additive and sialon z-value are critical as the results presented show. The optimum ceramic will comprise constituents which will give rise to little liquid formation during corrosion. The observation that the mullite forming $z = 3{\cdot}0$ material exhibits less liquid formation during corrosion in any of the environments investigated and that this is consistent with the lowest corrosion rates endorses such a design criterion.

5 Conclusions

(1) In general, the most corrosion resistant material in oxidising, chloridising, sulphidising and simulated gas environments at 1350°C is a $z = 3{\cdot}0$ sialon material.

(2) The presence of gaseous impurities (sulphur vapour, chlorine, hydrogen, sulphur dioxide, carbon dioxide) in the corrosion environments employed have the effect of increasing the volumes of liquid phase formed in the corrosion scales.

(3) The occurrence of increased volumes of liquid phase results in increased corrosion rates.

(4) The mechanism by which corrosion and indeed oxidation of silicon nitride–based ceramics occurs appears to involve the solution of sialon grains by such liquids, the extent and rates of liquid formation are controlled not only by the gaseous environment but also by cation diffusion effects.

Acknowledgements

The authors thank the commission of the European Communities for the grant given under BRITE-EURAM contract No. BREU/0180-C (EDB). The help rendered by Ms A. Flannery and Mr R. Bartley with regard to specimen fabrication and preparation is acknowledged.

References

1. Ekstrom, T. & Nygren, M., Sialon ceramics. *J. Am. Ceram. Soc.*, **75**(2) (1992) 259–76.
2. Blachere, J. R. & Pettit, F. S., *High Temperature Corrosion of Ceramics*, Noyes Data Corporation, Park Ridge, New Jersey, 1989.
3. Marra, J. E., Kriedler, E. R., Jacobson, N. S. & Fox, D. S., Reactions of silicon-based ceramics in mixed oxidation chlorination environments. *J. Am. Ceram. Soc.*, **71**(12) (1988) 1067–73.
4. Hsu, P., Sikyin, I., Park, C. & McNallan, M. J., Oxidation of silicon, silicon carbide and silicon nitride in gases containing oxygen and chlorine. *J. Am. Ceram. Soc.*, **76**(6) (1993) 1621–3.
5. Costa Oliveira, F. A., Edwards, R. A. H., Fordham, R. J. & De Wit, J. H. W., Factors limiting the application of silicon nitride ceramics in sulphur containing environments of low oxygen potential at high temperatures. In *Corrosion of Advanced Ceramics*, ed. K. G. Nickel, Kluwer Academic Publishers, 1994, pp. 177-88.
6. Sheehan, J. E., Passive and active oxidation of hot pressed silicon nitride materials with two magnesia contents. *J. Am. Ceram. Soc.*, **65** (1982) C111–4.
7. Costa Oliveira, F. A., Fordham, R. J. & De Wit, J. H. W., Degradation mechanisms of a silicon nitride in H_2–H_2O environments. In *Euroceramics II*, eds G. Ziegler & H. Hausner, Deutsche Keramische Gesellschaft e.V., 1991, pp. 1351–6
8. Martins, C. S., Steen, M. Bressers, J. & Rosa, L. G. High temperature flexure strength degradation of HP–Si_3N_4 pre-exposed to sulphidising aggressive environments. In *Euroceramics II*, eds G. Ziegler & H. Hausner, Deutsche Keramische Gesellschaft e.V., 1991, pp. 1357–61.
9. Demaison, J., Brossard, M., Demaison-Brut, M. & Goursat, P., Oxidation behaviour of β'-sialons in oxygen and carbon dioxide. In *Progress in Nitrogen Ceramics* ed. F. L. Riley, Martinus Nijhoff, The Hague, 1983, pp. 439–46.
10. Bouarroudj, A., Goursat, P. & Besson, J. L., Oxidation resistance and creep behaviour of a silicon nitride ceramic densified with Y_2O_3. *J. Mat. Sci*, **20** (1985) 1150–9.

11. Babini, G. N., Bellosi, A. & Vincenzini, P., A diffusion model for the oxidation of hot pressed Si_3N_4–Y_2O_3–SiO_2 materials. *J. Mat. Sci*, **19** (1984) 1029–42.
12. Pomeroy, M. & Hampshire, S., Oxidation processes in silicon-nitride-based ceramics. *Mat. Sci & Eng*, **A109** (1989) 389–94.
13. Pomeroy, M & Ramesh, R., Understanding the morphological development of oxidation products formed on β-sialon materials with different z-values. In *Microscopy of Oxidation-2*, eds S.B. Newcomb, & M. J. Bennett, Cambridge, UK, 1993, pp 566–75.
14. Ekstrom, T. & Olsson, P-O., β-sialon ceramics prepared at 1700°C by hot isostatic pressing. *J. Am. Ceram. Soc.*, **72**(9) (1989) 1722–4.
15. Bondar, A. & Galakov, F. Ya. In *Phase Diagrams for Ceramists*, ed. M. K. Reser, The American Ceramic Society, Columbus, Ohio, 1969, p. 165.
16. Daniel, P. L. & Rapp, R. A., Halogen corrosion of metals. In *Advances in Corrosion Science and Technology*, eds M. G. Fontana & R. W. Staehle, Plenum Press, NY, **6** 1976, pp. 55–72.
17. Hetherington, G., Jack, K. H., & Kennedy, J. C., The viscosity of vitreous silica. *Physics and Chemistry of Glasses*, **5**(5) (1964) 130–6.
18. Hampshire, S. & Jack, K. H., The kinetics of densification and, phase transformations of nitrogen ceramics. In *Special ceramics*, Vol. 7, eds P. Popper & D. E. Taylor, Proc. Brit. Ceram. Soc., **31** 1981, pp. 37.